DNS OF A CHANNEL FLOW WITH VARIABLE PROPERTIES

Franck Nicoud
Center for Turbulence Research, Stanford, CA94305-3030, USA
Thierry Poinsot
CERFACS, 31048 Toulouse Cedex, France

ABSTRACT

This paper describes Direct Numerical Simulations (DNS) of a low speed channel flow with strong heat transfer in the normal direction. The Reynolds number is of order 180 based on the channel half-height and the mean friction velocity. The low-Mach number approximation is applied to study the effects of density variations on turbulence. The data support the validity of the Van Driest (1951) transformation and suggest that the additive constant in the log law is a slight function of the heat flux parameter. A semi-local scaling is shown to be efficient for the streamwise turbulent fluctuations but not for the normal and spanwise turbulent intensities. Temperature fluctuations scale with the local mean temperature gradient.

MOTIVATIONS AND OBJECTIVES

The supersonic compressible turbulent boundary layer with or without heat transfer is well documented (see Bradshaw (1977), Fernholz and Finley (1980) and Spina et al. (1994) for reviews). Dimensional analysis of the inner layer shows that the law of the wall can be described in terms of two non-dimensional wall parameters, the friction Mach number $M_\tau = \frac{u_\tau}{c_w}$ and the heat flux parameter $B_q = \frac{q_w}{\rho_w C_p u_\tau T_w}$, where u_τ is the friction velocity $\sqrt{\tau_w \rho_w}$, c_w the speed of sound, q_w the heat flux, C_p the constant-pressure specific heat and T_w the temperature at the wall. Two cases $(M_\tau, B_q)=(0.08, -0.05)$ and $(0.12, -0.14)$ were considered in the DNS study of a supersonic channel flow performed by Coleman et al. (1995). These data were found in Huang and Coleman (1994) to support the validity of the Van Driest (1951) transformation

$$U^+_{VD} = \int_o^{u^+} \left(\frac{\rho}{\rho_w}\right)^{1/2} du^+ = \frac{1}{\kappa} \ln y^+ + C$$

and suggest that the additive constant C is a function of both M_τ and B_q.

The case with large heat transfer and small Mach number has received little attention. The usefulness of the Van Driest transformation to retrieve the classical logarithmic law of the wall is not fully accepted in this case (Cheng and Ng (1982), Wardana et al. (1994), Wang and Pletcher (1996)). A Large-Eddy Simulation of subsonic turbulent channel flow with constant heat flux performed by Dailey and Pletcher (1998) suggests that when the Mach number is close to 0 the constant C depends slightly on heat transfer. In their experiments, Wardana et al. (1994) study the effect of strong wall heating on turbulence statistics of a channel flow but do not use the Van Driest transformation to represent their mean velocity profiles.

The objective of the present work is to study the case where the thermo-physical properties vary significantly in the absence of compressibility effects ($M = M_\tau = 0$). We perform a DNS of a low speed flow with a large temperature gradient. The configuration is a plane channel flow between two isothermal walls with temperatures T_1 and T_2 (see Figure 1). The objective is to provide more reliable information about the variation of the constant of integration C as a function of B_q and to assess the existing scaling laws for the first order statistics.

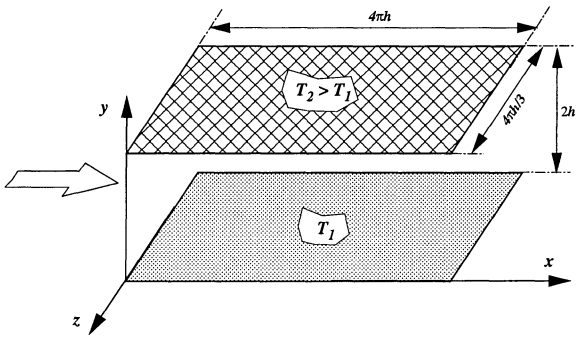

Figure 1: Computational domain.

EQUATIONS

To avoid contamination of the solution by the non-physical acoustic modes reported in Coleman et al. (1995), a low Mach number approximation is first applied to the 3D compressible Navier-Stokes equations. In doing so, the density is decoupled from the pressure so that no acoustics are present in the computation. This also eliminates the acoustic CFL restriction on the time step size.

To derive the low Mach number equations one expands the dependent variables as a power series in $\epsilon = \gamma M^2$, which is a small parameter (see Paolucci (1982) for a complete discussion). Substituting these expansions into the Navier-Stokes equations and collecting the lowest order terms in ϵ yields:

$$\frac{\partial \rho}{\partial t} + \frac{\partial \rho u_j}{\partial x_j} = 0 \tag{1}$$

$$\rho \frac{\partial u_i}{\partial t} + \rho u_j \frac{\partial u_i}{\partial x_j} = -\frac{\partial P}{\partial x_i} + \frac{1}{R_e} \frac{\partial \tau_{ij}}{\partial x_j} \tag{2}$$

$$\rho C_p \frac{\partial T}{\partial t} + \rho C_p u_j \frac{\partial T}{\partial x_j} = \frac{1}{R_e P_r} \frac{\partial q_j}{\partial x_j} + \frac{\gamma - 1}{\gamma} \frac{dP_o}{dt} \tag{3}$$

In these equations, all the variables are normalized using the reference state ρ^{ref}, u^{ref}, $T^{\text{ref}} = P_o^{\text{ref}}/\rho^{\text{ref}}$, $C_p^{\text{ref}} = C_p^*(T^{\text{ref}})$, $\mu^{\text{ref}} = \mu^*(T^{\text{ref}})$ and $k^{\text{ref}} = k^*(T^{\text{ref}})$ where the superscript * represent dimensional quantities. Also $R_e = \rho^{\text{ref}} u^{\text{ref}} L^{\text{ref}}/\mu^{\text{ref}}$ and $P_r = \mu^{\text{ref}} C_p^{\text{ref}}/k^{\text{ref}}$ are the Reynolds and Prandtl numbers while γ is the ratio of specific heats at the reference state. The non-dimensionalized velocity vector, density, temperature and specific heat are u_i, ρ, T and C_p whereas $\tau_{ij} = \mu \left(\frac{\partial u_i}{\partial x_j} + \frac{\partial u_j}{\partial x_i} - \frac{2}{3} \delta_{ij} \frac{\partial u_k}{\partial x_k} \right)$ and $q_j = k \frac{\partial T}{\partial x_j}$ are the viscous stress tensor and the heat flux vector respectively. The P in Eq. (2) may be interpreted as the hydrodynamic pressure. In the low-Mach number approximation, the thermodynamic pressure P_o only depends on time and must be computed if it is not constant. The equation of state is simply:

$$P_o = \rho T \tag{4}$$

Since density is uniquely determined by the temperature (and the thermodynamic pressure which is constant in space), the energy equation acts as a constraint which is enforced by the hydrodynamic pressure. Combining the equations (1), (3) and (4), this constraint is (in the case of a calorifically perfect gas):

$$\frac{\partial u_i}{\partial x_i} = \frac{1}{P_o(t) R_e P_r} \left[\frac{\partial q_j}{\partial x_j} - \frac{1}{V} \int_V \frac{\partial q_j}{\partial x_j} dV \right] \tag{5}$$

The time derivative of P_o is:

$$\frac{dP_o}{dt} = \frac{\gamma}{V} \frac{1}{R_e P_r} \int_V \frac{\partial q_j}{\partial x_j} dV = \frac{1}{V} \frac{1}{R_e P_r} \int_S q_j dS_j \tag{6}$$

and for a closed system, the total amount of mass M_0 is constant so that:

$$P_o(t) = \frac{M_0}{\int_V \frac{1}{T} dV} \tag{7}$$

NUMERICAL METHOD

The numerical method chosen for solving the variable density momentum and temperature equations is a generalization of a fully conservative fourth order spatial scheme developed for incompressible flows on staggered grids by Morinishi et al. (1998). It is fourth-order accurate in space, and third-order accurate in time. The algorithm is dissipation-free, and is thus well suited for DNS of turbulent flows. The key part is a Poisson equation with variable coefficient that is solved for the hydrodynamic pressure and that ensures that the proper constraint on the velocity field (Eq. 5) is recovered at the discrete level. It may be shown that this feature is needed to avoid violation of the conservation of kinetic energy in the inviscid limit which would otherwise arise through the pressure term in the momentum equation. The existing set of proper finite difference formulas for incompressible flow (Morinishi et al., 1998) is generalized to handle arbitrary large density fluctuations with no violation of conservation through the non-linear convective terms. The algorithm is virtually fully conservative (mass, momentum, kinetic energy). Several test cases were designed to check the accuracy of the method, including: **1)** 1D high-amplitude pulse of density in an inviscid flow, **2)** 1D small amplitude pulse of density in a viscous flow (analytical solution in Nicoud, 1998), **3)** 2D random fluctuations of velocity and temperature, **4)** 2D small amplitude fluctuations in a channel (growth rate compared to the linear stability theory by Suslov and Paolucci, 1995). More details can be found in Nicoud (1998).

Case	T_2/T_1	$R_{\tau 1} - R_{\tau 2}$	R_b	μ, k
A	1.01	182 – 185	2855	–
B	2	202 – 81	1786	Eq. 8
C	2	195 – 164	2810	$1/\sqrt{T}$
D	4	211 – 151	2818	$1/\sqrt{T}$

Table 1: DESCRIPTION OF THE DNS CASES.

Case	$10^3 C_{f1}$	$10^3 C_{f2}$	B_{q1}	B_{q2}
A	6.1	6.1	≈ 0	≈ 0
B	6.5	5.6	−0.018	+0.014
C	7.0	5.0	−0.018	+0.016
D	8.2	4.2	−0.041	+0.029

Table 2: FRICTION COEFFICIENTS AND HEAT FLUX PARAMETERS.

MEAN QUANTITIES

Details of the cases adopted are given in table 1 in which the indices '1' and '2' denote the cold and hot wall respectively. The bulk Reynolds number R_b is based on the bulk velocity and the values of density and dynamic viscosity corresponding to the bulk temperature. In Case A the temperature is almost uniform and the results may be compared to previous incompressible DNS performed by Kim and Moin (1987) and Kasagi (1992) as well as semi-empirical correlations derived by Kader (1981) for the passive scalar case. In Cases B-D one expects the temperature (density) variations to be large enough to modify the momentum balance through both viscous and inviscid effects. In Case B, the viscosity and diffusivity increase with temperature according to Sutherland's law:

$$k(T) = T^{3/2}\frac{1+S_k}{T+S_k}, \qquad \mu(T) = T^{3/2}\frac{1+S_\mu}{T+S_\mu} \quad (8)$$

with $S_k = 0.648$ and $S_\mu = 0.368$. Combining both the density and viscosity effects, the Reynolds number near the hot wall is much smaller than near the cold wall. The bulk Reynolds is also 30 % smaller than in the isothermal Case A. In an attempt to separate the Reynolds number effects from those of density gradients, Case B was redone by assuming that both the viscosity and the thermal diffusivity decrease when temperature increase viz. $\mu, k \propto 1/\sqrt{T}$. This kind of behavior would be relevant to a liquid. Table 1 shows that, with this inverse temperature dependance, the Reynolds number is almost independent of the temperature ratio (Cases C and D). The results for Case A do not depend on the functions $\mu(T)$ and $k(T)$ since the temperature varies only slightly in this case.

In each case the domain size is $(4\pi h, 2h, 4\pi/3h)$ and the grid contains 120x100x120 cells. The statistics were obtained over a time period of order $10h/\overline{u_\tau}$, where $\overline{u_\tau} = \frac{u_{\tau 1}+u_{\tau 2}}{2}$ is the mean friction velocity. The wall normal velocity points are distributed according to a hyperbolic tangent function for Cases A, C and D. For Case B, a non-symmetric distribution is used (Nicoud, 1998) consistent with the change in Reynolds number. The grid spacing in wall units is equivalent for all cases with $\Delta x^+ \approx 20$, $\Delta y^+_{\text{wall}} \approx 0.3$, $\Delta y^+_{\text{max}} \approx 9$ and $\Delta z^+ \approx 6$. The molecular Prandtl number is 0.76

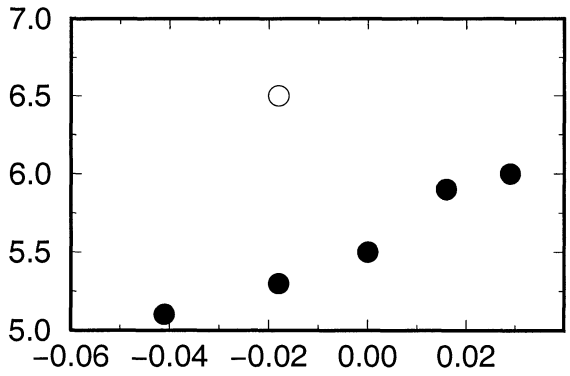

Figure 2: Additive constant C as a function of B_q for the transformed mean velocity profile. • : Cases A, C and D; ∘ : Case B

and buoyancy effects are neglected in all cases. An estimation of the ratio Gr/Re^2 (Gr is the Grashof number, $Re \approx 180$) for $\Delta T/T = 3/2$ (maximum value considered in the DNS's) with $\nu = 10^{-4}$ m^2/s as a typical value for hot dry air leads to $Gr/Re^2 \approx (35h)^3$. Thus the parameter Gr/Re^2 is small compared to unity (less than 5%) as long as h is smaller than 0.011 m. This means that the no-buoyancy assumption is justified if the characteristic length scale of the channel is of order 1 cm or less. This would be a reasonable range for a true experiment with temperature differences typical of a laboratory combustion chamber.

Table 2 gives the principal mean physical characteristics for Cases A-D. The friction coefficient is based on the mean density in the channel and the maximum velocity. The values obtained for the heat flux parameter B_q are small in absolute value compared to those in the DNS's of Coleman et al., 1995 ($B_q = -0.05$ and $B_q = -0.14$) although the mean channel centerline-to-wall temperature ratios are equivalent (1.5 for Case B-C and 2 for Case D, compared to 1.4 and 2.5 for the compressible channel flow). This is because the dissipation term in the internal energy equation is neglected in the low Mach number approximation.

Figure 2 shows the additive constant in the logarithmic law-of-the-wall for the transformed (as proposed

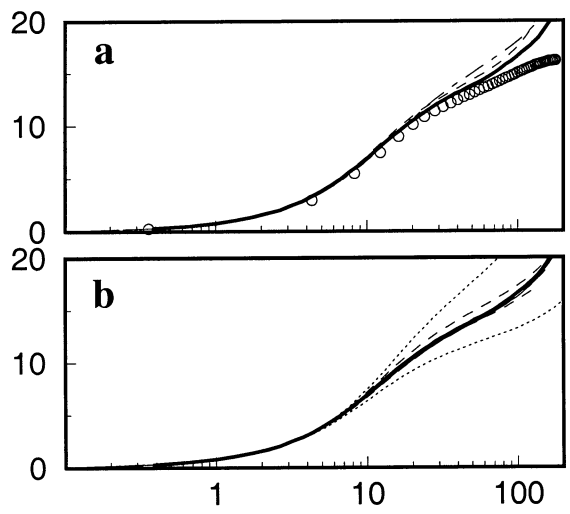

Figure 3: Mean velocity profiles. ——— : Passive scalar (Case A). (a): o : Kader's formula (1981); ——— : Case B, cooled side, plane (y^+,T^+); ····· : Case B, cooled side, plane (y^*,T^*). (b): ——— : Case C, both sides; ---- : Case D, both sides, plane (y^+,T^+); ····· : Case D, both sides, plane (y^*,T^*).

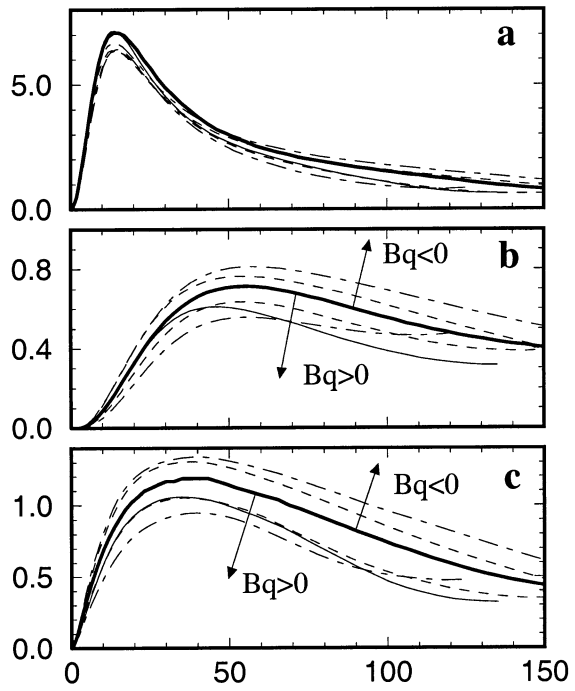

Figure 4: Turbulent fluctuations in semi-local scaling: (a): $\overline{u'^2}^*$, (b): $\overline{v'^2}^*$, (c): $\overline{w'^2}^*$. ——— : Passive scalar (Case A); ——— : Case B, cooled side; ---- : Case C, both sides; —·— : Case D, both sides.

by Van Driest, 1951) mean velocity profile as a function of the heat flux parameter B_q. Since the slope in the semi-log plot arises from local arguments in the fully turbulent region (P. Bradshaw, private communication), it is not supposed to depend on B_q. Accordingly, the values given in figure 2 were obtained by assuming $\kappa = 1/2.5$ (an accepted value for the channel flow at $R_\tau \approx 180$, Kim et al (1987)) and writing $C = U^+_{VD}(y^+ = 100) - 2.5\ln(100)$. The value of C for Case A is 5.5, in agreement with Kim et al. (1987). Both Cases C and D provide two values of C corresponding to the heated ($B_q > 0$) and the cooled ($B_q < 0$) side respectively. Figure 2 shows that all the values from Cases A, C and D suggest a slight increase of C with B_q whereas the value from the cooled side of Case B is clearly out of range due to the very low value of the bulk Reynolds number (see table 1). No data for $B_q > 0$ was deduced from this case due to the low value of $R_{\tau 2} < 100$. It follows that the reliable variations of C are of order 1, small enough to be neglected in first approximation. Indeed, a 10% change in friction coefficient corresponds to a change of about 1.3 in C (Bradshaw, 1977).

The mean temperature profiles for Case A and Case B are shown in figure 3a and a good agreement is found between the small temperature ratio Case A and Kader's formula (1981) for a passive scalar. The non-dimensionalization is such that that $T^+ = P_r y^+$ in the limit $y^+ \to 0$, viz. $T^+ = (T_w - T)/(B_q T_w)$ or $T^+ = (T_w - T)\rho_w C_p u_\tau / q_w$. The linear behavior for T near $y^+ = 180$ is related to the inflexion point near the centerline. Figure 3a also shows the cooled side of Case B with the same non-dimensionalization (y^+,T^+). A better collapse with Case A is obtained when a semi-local scaling is used, as suggested in Huang et al., 1995 (replacing ρ_w with $\rho(y)$, μ_w with $\mu(y)$ and $u_\tau = \sqrt{\tau_w/\rho_w}$ with $u^*_\tau(y) = \sqrt{\tau_w/\rho(y)}$ and then defining T^* and y^* in a similar manner as T^+ and y^+). The opposite situation is found when Cases A, C and D are compared instead. Figure 3b shows that the different curves collapse very well in the (y^+,T^+) plane whereas the semi-local non-dimensionalization does a poor job. Since $T^* = T^+\sqrt{\rho/\rho_w}$, the profiles $T^* = T^*(y^*)$ for the cooled and heated side of Case D are below and above the profile for the passive scalar case respectively. The reason why the wall scaling (y^+,T^+) leads to such a good collapse of the Cases A, C and D is still puzzling. It suggests that, except for the Reynolds number variation in the normal direction, the strength of the temperature difference does not modify the shape of the temperature profile.

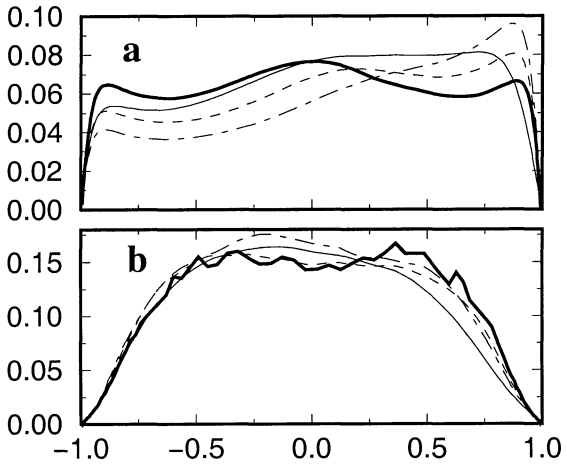

Figure 5: Temperature fluctuations in global coordinates. (a): scaling is $T_2 - T_1$; (b): scaling is $2h \times |\partial\overline{T}/\partial y|$. ——— : Passive scalar (Case A); ——— : Case B; - - - - : Case C; —·— : Case D.

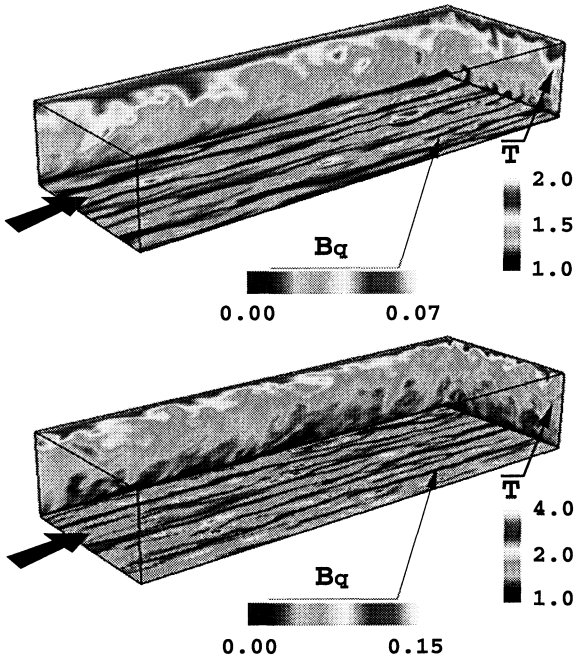

Figure 6: Flow field visualization. Flow is from left to right. **Top:** Case A. **Bottom:** Case D.

TURBULENT FLUCTUATIONS

Figure 4 shows the turbulent intensities in the streamwise (a), normal (b) and spanwise (c) directions for the different cases. It was shown in Nicoud (1998) that the results for Case A are in very good agreement with Kim et al. (1987). For the other cases, the better scaling was found to be the semi-local one. Figure 4a shows that all the curves collapse within to a few percent as far as the streamwise fluctuations are concerned. However, the scaling is not as good for the normal and the spanwise components (although it is better than the wall scaling). A difference in the maximum of $\overline{v'^2}^*$ (figure 4b) and $\overline{w'^2}^*$ (figure 4c) as high as 35% (between the two extreme cases considered: cooled and heated sides of Case D) is found. In both cases, the more negative or positive the heat flux parameter is, the larger or smaller the stress becomes. This is however not true when the Reynolds number changes in the normal direction (Case B, cooled side). The semi-local scaling remains efficient for the streamwise component but the normal and spanwise fluctuations are smaller than in the passive scalar case, even if the heat flux parameter is negative. However, as mentioned in the previous section, the Reynolds number in Case B is so low that the comparison with Case A may not be relevant.

Figure 5 shows that the temperature fluctuations scale better when the local mean temperature gradient is used instead of the temperature difference $T_2 - T_1$. Particularly, the heat flux fluctuations at the wall ϕ_{rms} scale with the mean wall heat flux $< \phi >$ and the absolute value of the ratio

$$\phi_{\rm rms} / < \phi > \qquad \text{(assessed at the walls)}$$

is in the range $0.385 - 0.4$ in all cases (Kim and Moin (1987) found 0.396 for the passive scalar case). The mean gradient-based scaling also supports the definition of the integral thermal length scale $l_T \propto T_{rms}/|\partial\overline{T}/\partial y|$ as used by Gaviglio (1987) to build its analogy. The results suggest $\frac{T_{\rm rms}}{u_{\rm rms}} \frac{|\partial\overline{u}/\partial y|}{|\partial\overline{T}/\partial y|} = R_0$ with $R_0 \approx 1.34$ on the cold sides (value proposed by Rubesin, 1990) whereas $R_0 \approx 1.15 - 1.20$ on the hot side (in better agreement with Huang et al., 1995). Also, the results do not show dramatic changes in the turbulent Prandtl number, even for high temperature ratios. They support the usual assumption $P_{\rm rt} \approx 0.9$ fairly well (not shown).

VISUALIZATION

As previously stated, the Reynolds number on the heated side of the channel becomes very low if the molecular viscosity evolves according to Sutherland's law. Consequently the size of the turbulent structures are much higher near the hot wall in Case B (see figure 6, top). The characteristic length scale of the turbulence is basically the same on the two sides of the channel if both the dynamic viscosity and the diffusivity

decrease with temperature as $1/\sqrt{T}$ (see figure 6, bottom). In all cases the streamwise velocity-temperature correlation coefficient is very high near the walls (of order 0.95, as in the previous studies for passive scalar, Kim and Moin (1987), Kasagi (1992)). Subsequently the wall heat flux reveals the elongated streaky structure of turbulence. The temperature field is also a good marker for the bursting events already observed in previous studies of isothermal flows. The examination of higher-order statistics (e.g. the skewness factor of the u) suggests that the ejection of low-speed fluid is intensified on the heated side (Nicoud, 1998). This is in agreement with the experimental finding of Wardana et al. (1994). Further work is needed to clarify this modification on the turbulence structure.

CONCLUSION

Direct Numerical Simulations of the effects of variable density and molecular viscosity on a channel flow between two isothermal walls have been performed for three different temperature ratios $(1-4)$ and two different viscosity laws. The results support the Van Driest transformation for the mean velocity profile as well as a semi-local scaling for the streamwise velocity fluctuations. However, neither the normal nor the spanwise turbulent intensities scale properly with the semi-local friction velocity $\sqrt{\tau_w}/\rho$. The better scaling for the temperature fluctuations is based on the local mean temperature gradient. Further work is needed to clarify the physical effect of the mean density gradient.

REFERENCES

Bradshaw P., 1977, Compressible turbulent shear layers, *Ann. Rev. Fluid Mech.*, Vol. 9, pp.33-54

Cheng R.K. and Ng T.T., 1982, Some aspects of strongly heated turbulent boundary layers flows, *Phys. Fluids*, Vol. 25, No. 8, pp.1333-1341

Coleman G. N., Kim J., and Moser R. D., 1995, A numerical study of turbulent supersonic isothermal-wall channel flow, *J. Fluid Mech*, Vol. 305, pp.159-183.

Dailey L.D. and Pletcher R.H., 1998, Large eddy simulation of constant heat flux turbulent channel flow with property variations, AIAA 98-0791, Reno, January 12-15

Fernholz H.H. and Finley P.J., 1980, A critical commentary on mean flow data for two-dimensional compressible turbulent boundary layers, AGARD-AG-253

Gaviglio J., 1987, Reynolds analogies and experimental study of heat transfer in the supersonic boundary layer, *Int. J. Heat Mass Transfer*, Vol. 30, No. 5, pp.911-926

Huang P.G. and Coleman G.N., 1994, Van Driest transformation and compressible wall-bounded flows, *AIAA J.*, Vol. 32, No. 10, pp.2110-2113

Huang P.G., Coleman G.N. and Bradshaw P., 1995, Compressible turbulent channel flows: DNS results and modeling, *J. Fluid Mech.*, Vol. 305, pp.185-218

Kader B., 1981, Temperature and concentration profiles in fully turbulent boundary layers, *Int. J. Heat Mass Transfer*, Vol. 24, No. 9, pp.1541-1544

Kasagi N., Tomita Y. and Kuroda A., 1992, Direct numerical simulation of the passive scalar field in a turbulent channel flow, *ASME J. Heat Transfer*, Vol. 114, pp.598-606

Kim J., Moin P. and Moser R., 1987, Turbulence statistics in fully developed channel flow at low Reynolds number, *J. Fluid Mech.*, Vol. 177, pp.133-166

Kim J. and Moin P., 1987, Transport of passive scalars in a turbulent channel flow, Turbulent Shear flows 6, pp.85-96

Morinishi Y., Lund T., Vasilyev O. and Moin P., 1998, Fully Conservative higher order finite difference schemes for incompressible flow, *J. Comp. Phys.*, Vol. 143, No. 1, pp.90-124

Nicoud F., 1998, Numerical study of a channel flow with variable properties, Center for Turbulence Research, CTR Annual Research Briefs, pp.289-310.

Paolucci S. , 1982, On the filtering of sound from the Navier-Stokes equations, SAND82-8253, Sandia National Laboratories, Livermore.

Rubesin M.W., 1990, Extra compressibility terms for Favre-averaged two-equation models of inhomogeneous turbulent flows, NASA CR-177556.

Spina E.F., Smits A.J. and Robinson S.K., 1994, The physics of supersonic turbulent boundary layers, *Ann. Rev. Fluid Mech.*, Vol. 26, pp.287-319

Suslov S. and Paolucci S. , 1995, Stability of mixed-convection flow in a tall vertical channel under non-Boussinesq conditions, *J. Fluid Mech*, Vol. 302, pp.91-115.

Van Driest E.R., 1951, Turbulent boundary layers in compressible fluids, *J. Aero. Sci.*, Vol. 18, No. 3, pp.145-160

Wang W. and Pletcher R., 1996, On the large eddy simulation of a turbulent channel flow with significant heat transfer, *Phys. Fluids*, Vol. 8, No. 12, pp.3354-3366

Wardana I.N.G., Ueda T. and Mizomoto M., 1994, Effect of strong wall heating on turbulence statistics of a channel flow, *Experiments in Fluids*, Vol. 18, pp.87-94